

# The two electron artificial molecule

B. Partoens,<sup>1\*</sup> A. Matulis,<sup>2◊</sup> and F. M. Peeters<sup>1†</sup>

<sup>1</sup>Departement Natuurkunde, Universiteit Antwerpen (UIA), Universiteitsplein 1, B - 2610 Antwerpen, Belgium

<sup>2</sup>Semiconductor Physics Institute, Goštauto 11, 2600 Vilnius, Lithuania

(March 17, 2018)

Exact results for the classical and quantum system of two vertically coupled two-dimensional single electron quantum dots are obtained as a function of the interatomic distance ( $d$ ) and with perpendicular magnetic field. The classical system exhibits a second order structural transition as a function of  $d$  which is smeared out and shifted to lower  $d$  values in the quantum case. The spin-singlet  $\leftrightarrow$  spin-triplet oscillations are shifted to larger magnetic fields with increasing  $d$  and are quenched for a sufficiently large interatomic distance.

PACS numbers: 73.20.Dx, 36.40.Ei, 64.90.+b

Quantum dots are *artificial atoms* which have been a subject of intense theoretical and experimental research in recent years [1]. A very recent development is the study of vertically coupled quantum dots [2] or *artificial molecules*. In Ref. [3] a double dot system containing three spin-polarized electrons was investigated. A sequence of angular momentum magic numbers was found which depends on the strength of the interdot tunneling. An analytically solvable model of an arbitrary number of vertically coupled quantum dots containing each two electrons but with a  $1/r^2$  electron-electron interaction and with neglect of the interdot tunneling was presented in Ref. [4]. The first experimental realization of vertically coupled quantum dot structures were recently reported [5,6].

Two vertically coupled *classical* dots were investigated by two of the present authors as a function of the interatomic distance ( $d$ ) [7]. We found first and second order transitions which are similar to structural phase transitions. For first (second) order transitions the first (second) derivative of the energy with respect to  $d$  is discontinuous, the radial position of the particles changes discontinuously (continuously), and the frequency of the eigenmodes exhibits a jump (one mode becomes soft, i.e., its frequency becomes zero). Here we will investigate the influence of quantum effects on the above structural transitions. As an example we limit ourselves to the exact solvable artificial molecule with in each dot one electron. In the classical limit this system exhibits a second order transition. We also investigate how the spin-singlet  $\leftrightarrow$  spin-triplet oscillations are modified by changing the interatomic distance. The equivalent two electron quantum dot, i.e.  $d = 0$ , was solved in Refs. [8–10]. We will show that the inter-layer distance introduces an additional parameter with which the electron-electron interaction can

be altered, and which modifies the behavior of the system considerably.

The present system consists of two layers, separated in the  $z$ -direction by a distance  $d$ , with in each layer ( $xy$ -plane) one electron which is confined by a parabolic potential. We take the same confinement strength in both layers and the barrier between the two layers is taken sufficiently large such that there is no tunneling between them. Within the effective mass approximation, this system is described by the following Hamiltonian

$$H_t = \frac{1}{2m} \sum_{i=1}^2 \left( \vec{p}_i + \frac{e}{c} \vec{A}(\vec{r}_i) \right)^2 + U(\vec{r}_1, \vec{r}_2), \quad (1)$$

$$U(\vec{r}_1, \vec{r}_2) = \frac{1}{2} m \omega_0^2 (r_1^2 + r_2^2) + \frac{e^2}{\epsilon} \frac{1}{\sqrt{|\vec{r}_1 - \vec{r}_2|^2 + d^2}}, \quad (2)$$

with  $m$  the effective electron mass,  $\epsilon$  the dielectric constant of the medium the electrons are moving in, and  $\omega_0$  the radial confinement frequency. A magnetic field is applied perpendicular to the dots,  $\vec{B} = B\vec{e}_z$ , which in the symmetric gauge is described by the vector potential  $\vec{A}(\vec{r}) = [\vec{B} \times \vec{r}]/2$ , and the above Hamiltonian can be rewritten as follows

$$H_t = \frac{1}{2m} (p_1^2 + p_2^2) + \tilde{U}(\vec{r}_1, \vec{r}_2) - \frac{1}{2} \omega_c \{ [\vec{p}_1 \times \vec{r}_1] + [\vec{p}_2 \times \vec{r}_2] \}_z, \quad (3)$$

where the symbol  $\omega_c = eB/mc$  stands for the cyclotron frequency and the potential  $\tilde{U}$  is given by expression (2) with the scaled confinement frequency  $\tilde{\omega}_0 = \gamma\omega_0$  where  $\gamma = \sqrt{1 + \omega_c^2/4\omega_0^2}$ .

A crucial property of parabolic confinement potentials is that the center-of-mass and the relative motion are separable. The center-of-mass coordinate and the relative coordinate are  $\vec{R} = (\vec{r}_1 + \vec{r}_2)/2$  and  $\vec{r} = \vec{r}_1 - \vec{r}_2$ , respectively, with the conjugate momenta  $\vec{P} = \vec{p}_1 + \vec{p}_2$  and  $\vec{p} = (\vec{p}_1 - \vec{p}_2)/2$ . The center-of-mass and relative motions are described by the following Hamiltonians

$$W(\vec{P}, \vec{R}) = \frac{1}{4m} P^2 + m\omega_0^2 R^2 - \frac{1}{2} \omega_c [\vec{P} \times \vec{R}]_z, \quad (4a)$$

$$H(\vec{p}, \vec{r}) = \frac{1}{m} p^2 + \tilde{U}(r) - \frac{1}{2} \omega_c [\vec{p} \times \vec{r}]_z, \quad (4b)$$

where

$$U(r) = \frac{1}{4} m \omega_0^2 r^2 + \frac{e^2}{\epsilon} \frac{1}{\sqrt{r^2 + d^2}}, \quad (5)$$

and  $\tilde{U}$  is obtained from  $U$  by replacing  $\omega_0$  by  $\tilde{\omega}_0$ .

In the following we do not have to consider the center-of-mass motion because it is a harmonic oscillator with ground-state energy and excitation frequencies which do not depend on the interatomic distance  $d$ . We concentrate our attention on the relative motion.

First we consider the classical problem. The Newton equation of motion for this system is

$$\ddot{\vec{r}} = [\tilde{\omega}_c \times \dot{\vec{r}}] - \frac{2}{m} \nabla U(\vec{r}), \quad (6)$$

with  $\tilde{\omega}_c = \omega_c \vec{e}_z$ . The classical ground-state configuration is obtained by minimizing the potential  $U(\vec{r})$ . A second order transition occurs when the Coulomb interaction energy and the confinement energy are of the same order. To emphasize this we write the Hamiltonian in dimensionless form where we express the coordinates and energy in the following units  $r' = (e^2/\epsilon)^{1/3} \alpha^{-1/3}$  and  $E' = (e^2/\epsilon)^{2/3} \alpha^{1/3}$ , respectively, with  $\alpha = m\omega_0^2/2$ . The potential reduces to

$$U(r) = \frac{1}{2}r^2 + \frac{1}{\sqrt{r^2 + d^2}}, \quad (7)$$

which after minimalisation leads to the equilibrium radius for the ground-state configuration  $r_0(d) = \sqrt{1 - d^2}$  for  $d < 1$ , and  $r_0(d) = 0$  for  $d > 1$ . The corresponding energy, and its first and second derivatives with respect to the distance  $d$  are  $E = (3 - d^2)/2$ ,  $\partial E/\partial d = -d$  and  $\partial^2 E/\partial d^2 = -1$  for  $d < 1$ , and  $E = 1/d$ ,  $\partial E/\partial d = -1/d^2$  and  $\partial^2 E/\partial d^2 = 2/d^3$  for  $d > 1$ . The first and second derivatives are shown in Fig. 1 by the dashed curves. It is clear that there is a second order transition at  $d = 1$ . This second order transition is of the same type as the single second order transitions we found previously for the artificial molecules with twice six, seven and eight electrons [7].

Next we calculate the frequencies of the eigenmodes. We express the frequencies in the unit  $\omega' = \omega_0/\sqrt{2}$  and the equation of motion becomes

$$\ddot{\vec{r}} = [\tilde{\omega}_c \times \dot{\vec{r}}] - 2\nabla U(\vec{r}), \quad (8)$$

where the dimensionless potential (7) is used. To find the spectrum we take the Fourier transform of this Newton equation which leads to the following excitation frequencies

$$\begin{aligned} \omega_r &= 0, \quad \omega_b = \sqrt{6(1 - d^2) + \omega_c^2}, & d < 1; \\ \omega_{\pm} &= \sqrt{2(1 - 1/d^3) + (\omega_c/2)^2} \pm \omega_c/2, & d > 1. \end{aligned} \quad (9)$$

The frequency  $\omega_r = 0$  corresponds to the rotation of the molecule as a whole, and  $\omega_b$  is the frequency of the breathing mode. The frequencies  $\omega_+$  and  $\omega_-$  correspond with the out-of-phase motions of the electrons around the center of the dots. These classical frequencies are shown in Fig. 2 for  $\omega_c = 0$  by the dashed curves. Note that

one of the eigenmodes softens at  $d = 1$  which induces the second order transition.

Now we turn our attention to the quantum mechanical problem and investigate how quantum effects influence the classical transition. In the quantum case the ground-state energy can be obtained as a solution of the Schrödinger equation. Due to the cylindrical symmetry of the problem it reduces to the following equation for the radial wave function ( $\Psi(\vec{r}) = \exp(-im\varphi)R_m(r)$ )

$$\left\{ -\lambda^2 \left( \frac{1}{r} \frac{d}{dr} r \frac{d}{dr} \right) + \frac{\lambda^2 m^2}{2} - \lambda \frac{\omega_c}{2} m + \tilde{U}(r) - E \right\} R_m(r) = 0 \quad (10)$$

where

$$\tilde{U}(r) = \frac{\gamma^2}{2} r^2 + \frac{1}{\sqrt{r^2 + d^2}}, \quad (11)$$

and  $\lambda = \hbar\omega_0/(\alpha r'^2 \sqrt{2})$ , which is the ratio of the quantum energy with the energy at the transition point. We solved this differential equation numerically, using a non uniform space grid as was done in Ref. [11].

To see how quantum effects influence the classical transition at  $d = 1$  we solve Eq. (10) for  $\omega_c = 0$  and we take  $\lambda$  slightly different from 0. In Fig. 1(a) the first and second derivative of the ground-state energy (i.e.  $n = 0$ ,  $m = 0$ ) with respect to  $d$  is given for  $\lambda = 10^{-4}$ , together with the classical result. Fig. 1(b) shows the same results for  $\lambda = 0.2$ . One notices that quantum fluctuations smear out the classical transition which happens already for very small values of  $\lambda$ . In order to reveal the influence of the quantization on the eigenfrequencies obtained classically we define them in the quantum case as the smallest differences between the excited state energies of Eq. (10) divided by  $\lambda$ . This is shown in Fig. 2 for  $\lambda = 10^{-2}$ . In agreement with the disappearance of the classical transition there is no softening of a frequency mode in the quantum case.

The effects of these quantum fluctuations can be understood from a simple qualitative consideration. As we are interested in the behavior of the system close to the transition point we use the following expansion of the potential (11)

$$\tilde{U}(r) = \frac{1}{2} \left( \gamma^2 - \frac{1}{d^3} \right) r^2 + \frac{3r^4}{8d^5} \sim \frac{3}{2} \Delta d r^2 + \frac{3}{8} r^4, \quad (12)$$

where we neglect the constant shift and introduced the parameter  $\Delta d = (d - \tilde{d}_0)\gamma^{8/3}$ , which characterizes the deviation from the exact transition point  $\tilde{d}_0 = \gamma^{-2/3} \approx 1 - \omega_c^2/12\omega_0$ . Thus in the quantum case the magnetic field shifts the transition point to lower  $d$  values.

After the above expansion we arrive at the following radial equation which describes the quantum behavior of the system for small  $\lambda$  values and close to the transition point

$$\left\{ -\lambda^2 \left( \frac{1}{r} \frac{d}{dr} r \frac{d}{dr} \right) + \frac{\lambda^2 m^2}{r^2} + \frac{3}{2} \Delta d r^2 + \frac{3}{8} r^4 - E \right\} R_m(r) = 0. \quad (13)$$

Note that there are two parameters  $d$  and  $\lambda$  which control the quantum problem while in the classical case there is only one parameter  $d$  which controls the closeness to the transition point. The role of the other parameter  $\lambda$  can be understood by considering the following limiting cases, where we take  $\omega_c = 0$  for simplicity. In the case when the parameter  $\Delta d$  is not too small one may neglect the quartic term in Eq. (13) and we obtain the Schrödinger equation for a harmonic oscillator. This leads to the following excitation frequency estimation  $\omega \sim E/\lambda \sim \sqrt{\Delta d}$ . Consequently, not too close to the transition point the excitation frequency demonstrates the classical soft mode behavior. In the opposite limiting case close to the transition point (small  $\Delta d$  values) the quadratic term can be neglected. Scaling the variable  $r \rightarrow \lambda^{1/3} r$  it can be estimated that the excitation frequencies are of order  $\omega \sim E/\lambda \sim \lambda^{1/3}$ . Therefore, in the quantum case the soft mode frequency does not tend to zero, as is also apparent in Fig. 2. Comparing the frequency estimations in both  $\Delta d$  regions we find that in the region  $|\Delta d| < \lambda^{2/3}$  quantization influences the classical transition point behavior. For  $\lambda = 10^{-4}$ , as in Fig. 1(a), this region is about  $\Delta d \approx 10^{-2}$ , which agrees with the numerical results of Fig 1(a).

From Fig. 1 we also notice that in the quantum case the transition is shifted to smaller  $d$  values. As a measure for this shift we take the interatomic distance value at which  $\partial E/\partial d$  attains its minimum value for the ground-state energy ( $n = 0$ ,  $m = 0$ ). This interatomic distance (thick curve in Fig. 3) coincides almost with the  $d$  value (dashed curve in Fig. 3) at which the radial wavefunction (inset of Fig. 3) becomes maximal in the center of the dot. The shift of the transition to smaller  $d$  values can also be induced by applying an external magnetic field (see Fig. 3). The plotted results for  $\omega_c = 5$  are also for the state ( $n = 0$ ,  $m = 0$ ), which is not the ground-state anymore, except for large  $d$  values. Thus in the quantum case the electrons sit in the center of both dots for smaller  $d$  values than in the classical case, which causes the shift to lower  $d$  values.

It is known that in quantum dots [9] and in the  $D^-$  problem [12] oscillations between spin-singlet and spin-triplet ground-states occur as a function of the magnetic field strength. Here we want to investigate how these oscillations change when the distance between the dots increases and how they are altered or modified by the presence of the classical transition. It is obvious that when the interatomic distance  $d$  increases, a higher magnetic field is needed to induce these transitions and that for sufficiently large  $d$  no transitions occur.

In Fig. 4(a) these spin-singlet  $\leftrightarrow$  spin-triplet oscilla-

tions are shown for  $d = 0.5$  and  $\lambda = 0.1$ . In Fig. 4(b) we plot the phase diagram for the system with  $\lambda = 0.1$ . When  $d$  increases, the transitions are shifted to higher magnetic fields. The classical transition is seen as follows: for  $d > 1$  we found no spin-singlet  $\leftrightarrow$  spin-triplet transitions anymore, while for  $d < 1$  oscillations do occur and this for all values of  $\lambda$ . As in the classical system, the interlayer correlations are sufficiently strong to impose the one atom properties for  $d < 1$ , and for  $d > 1$  the system behaves like two decoupled quantum dots. The spin-singlet  $\leftrightarrow$  spin-triplet oscillations in quantum dots are related to the Wigner crystallization state of the quantum dot [13,14] what in our case corresponds to the transition at  $d = 1$  and which explains why for  $d > 1$  those oscillations are absent.

Acknowledgments. B.P. is a research assistant and F.M.P. a research director with the Flemisch Science Foundation (FWO-Vlaanderen). Part of this work is supported by IUAP-IV and FWO-Vlaanderen.

---

\* Electronic address: bpartoen@uia.ua.ac.be

◊ Permanent address: Semiconductor Physics Institute, Goštauto 11, 2600 Vilnius, Lithuania. Electronic address: matulis@pub.osf.lt

† Electronic address: peeters@uia.ua.ac.be

- [1] *Quantum dots*, L. Jacak, P. Hawrylak, and A. Wójs (Springer-Verlag Berlin Heidelberg, 1998).
- [2] J. J. Palacios and P. Hawrylak, Phys. Rev. B **51** 1769 (1995).
- [3] H. Imamura, P. A. Maksym, and H. Aoki, Phys. Rev. B **53**, 12613 (1996).
- [4] S. C. Benjamin and N. F. Johnson, Phys. Rev. B **51**, 14733 (1995).
- [5] D. G. Austing, T. Honda, K. Muraki, Y. Tokura, and S. Tarucha, Physica B **249**, 206 (1998).
- [6] G. S. Solomon, J. A. Trezza, A. F. Marshall, and J. S. Harris, Jr., Phys. Rev. Lett. **76**, 952 (1996).
- [7] B. Partoens, V. A. Schweigert, and F. M. Peeters, Phys. Rev. Lett. **79**, 3990 (1997).
- [8] U. Merkt, J. Huser, and M. Wagner, Phys. Rev. B **43**, 7320 (1991).
- [9] M. Wagner, U. Merkt, and A. V. Chaplik, Phys. Rev. B **45**, 1951 (1992).
- [10] J.-J. S. De Groote, J. E. M. Hornos, and A. V. Chaplik, Phys. Rev. B **46**, 12773 (1992).
- [11] F. M. Peeters and V. A. Schweigert, Phys. Rev. B **53**, 1468 (1996).
- [12] C. Riva, V. A. Schweigert, and F. M. Peeters, Phys. Rev. B **57**, 15392 (1998).
- [13] P. A. Maksym, Phys. Rev. B **53**, 10871 (1996).
- [14] E. Anisimovas and A. Matulis, J. Phys.: Condens. Matter **10**, 601 (1996).

FIG. 1. The first and second derivative (full curves) of the ground-state energy for  $\omega_c = 0$ , i.e.  $n = 0, m = 0$ , for the quantum artificial molecule as a function of  $d$  for (a)  $\lambda = 10^{-4}$  and (b)  $\lambda = 0.2$ . The classical result ( $\lambda = 0$ ) is shown by the dashed curves.

FIG. 2. The quantum mechanical frequencies (full curves) for  $\lambda = 10^{-2}$  and the classical frequencies (dashed curves) as a function of  $d$  and for  $\omega_c = 0$ .

FIG. 3. The dashed curve is the  $d$  value for which  $\partial E/\partial d$  is minimal, which is a measure for the shift of the transition. The full curve is the minimum  $d$  value at which the radial wavefunction (inset of figure) attains a maximum at  $r = 0$ . The results are shown for  $\omega_c = 0$  and  $\omega_c = 5$ .

FIG. 4. (a) The lowest energy levels for the two-electron double quantum dot problem ( $d = 0.5, \lambda = 0.1$ ). The singlet phase  $m = 0$  ( $S = 0$ ) at low magnetic fields is followed by  $m = 1$  ( $S = 1$ ),  $m = 2$  ( $S = 0$ ), ... phases as the magnetic field strength is increased. (b) Phase diagram for singlet and triplet ground-states for  $\lambda = 0.1$ . Only the first eight transitions are shown. When  $d > 1$  no transitions occur.

Figure 1

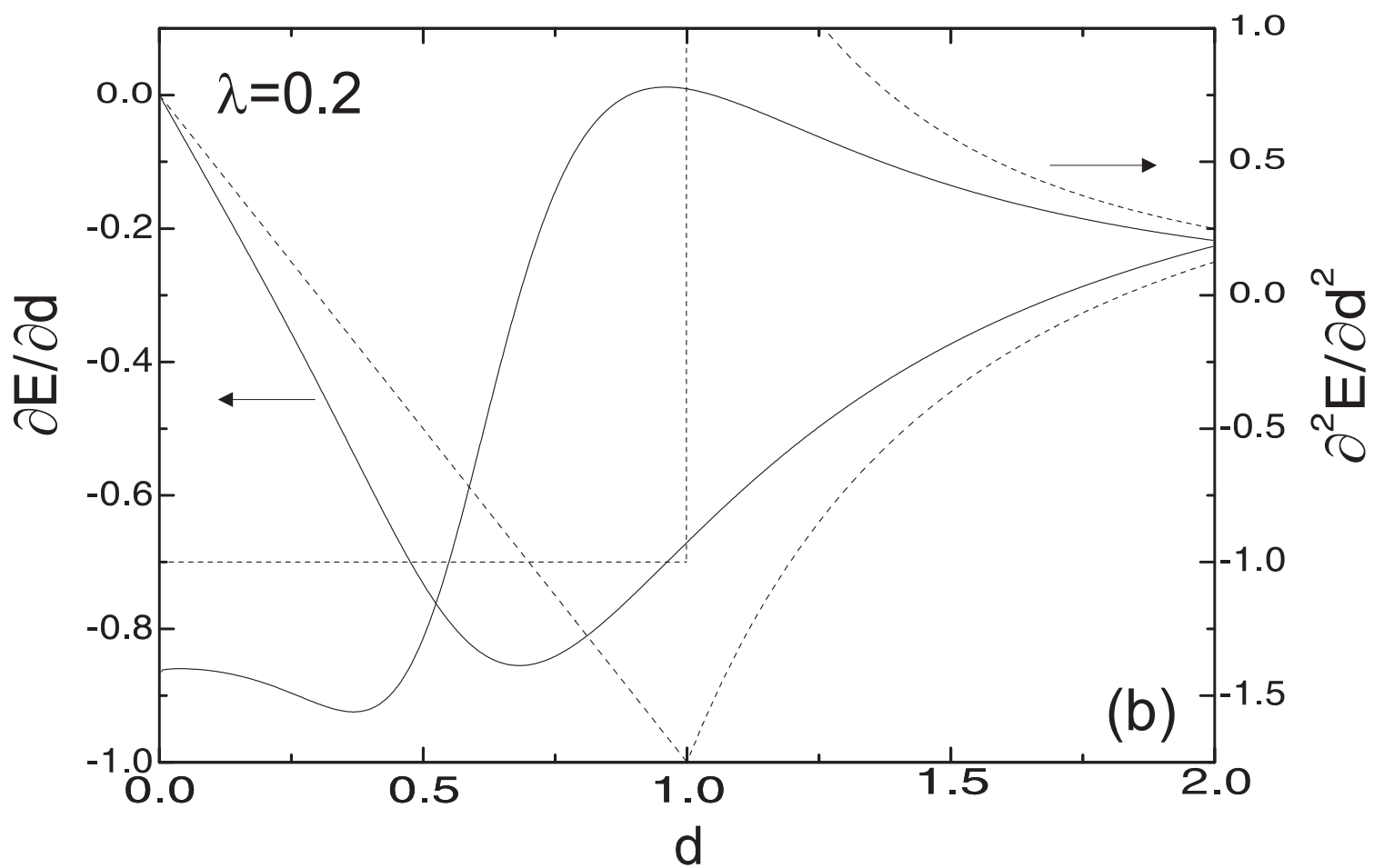
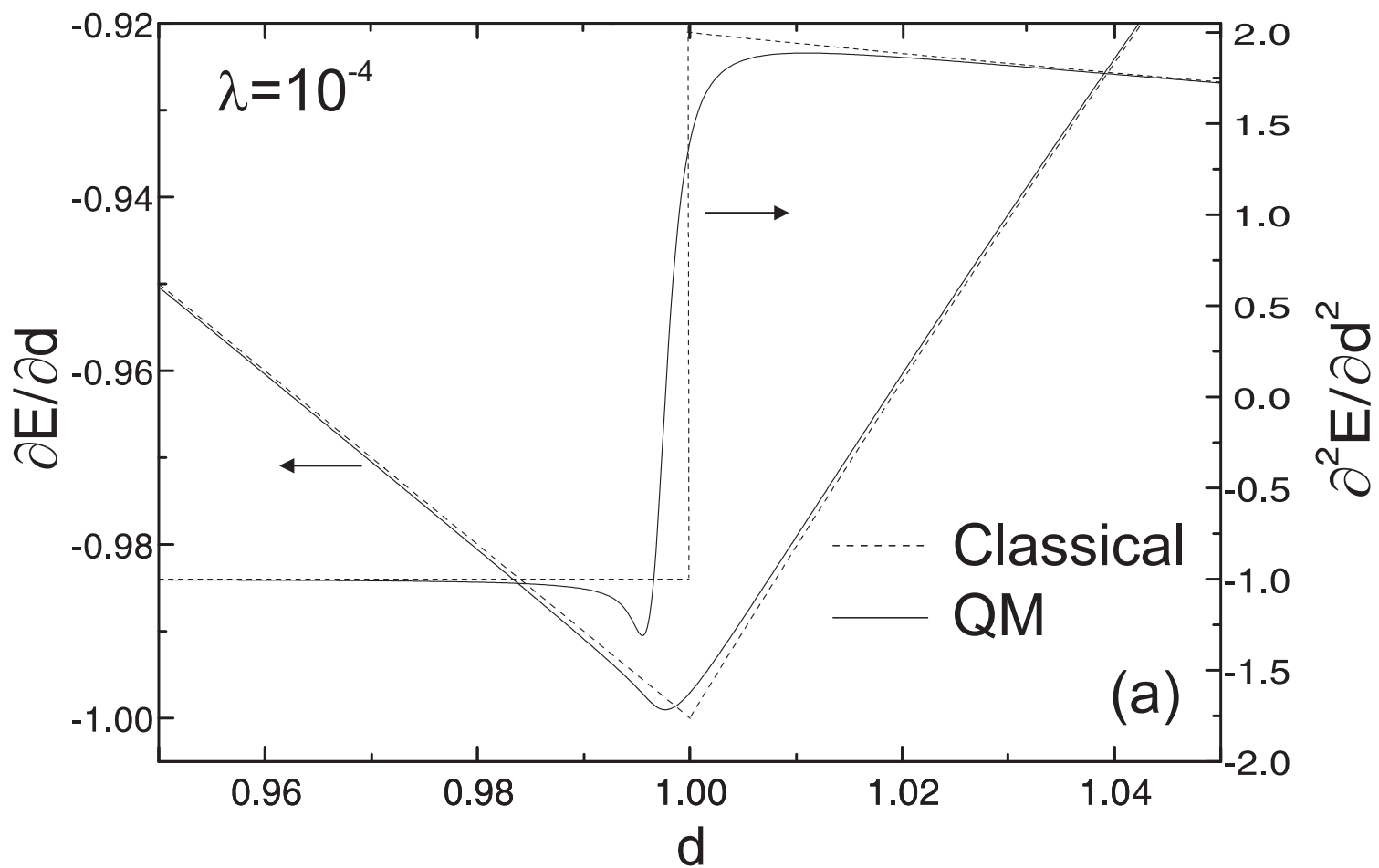


Figure 2

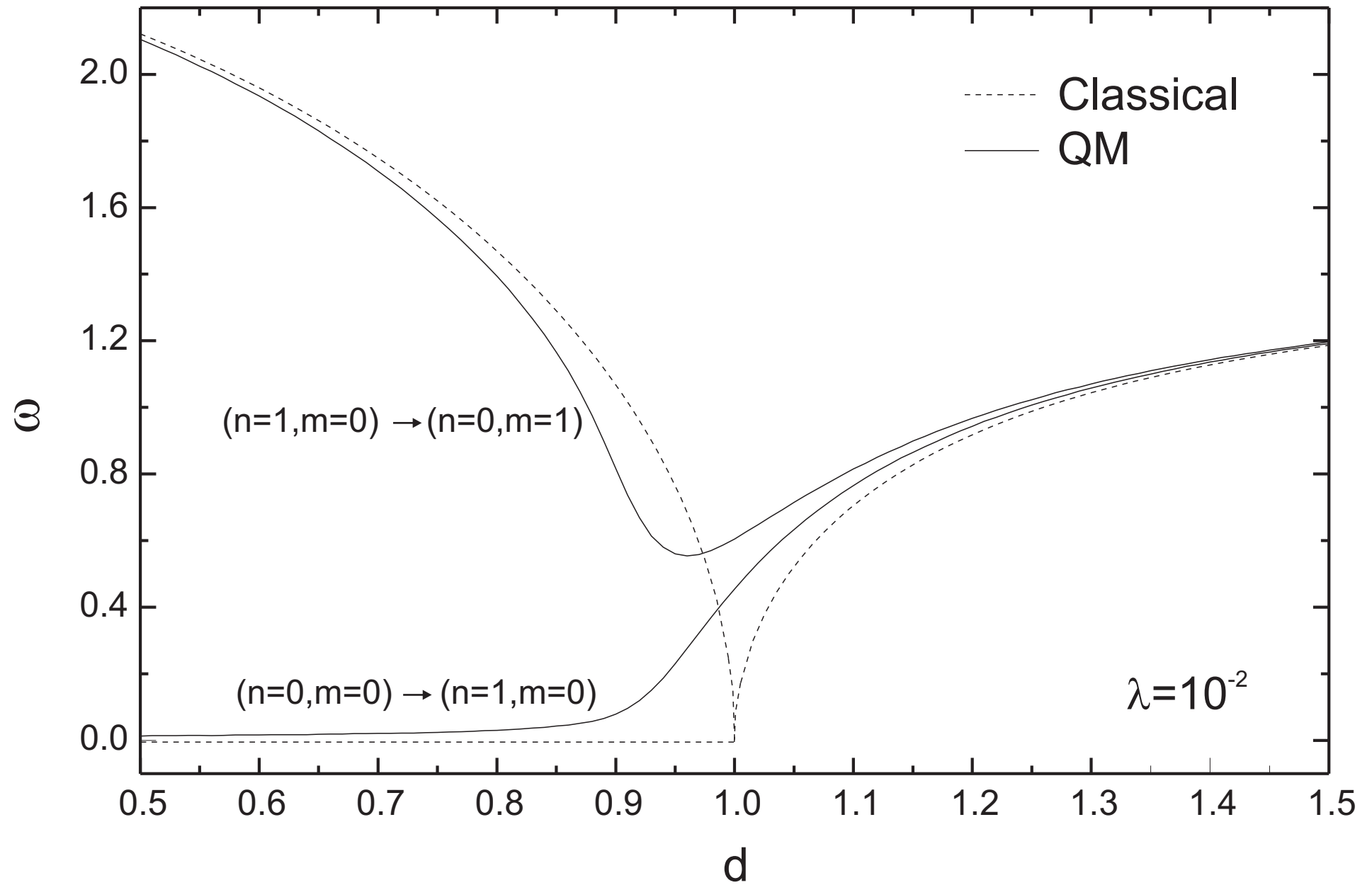


Figure 3

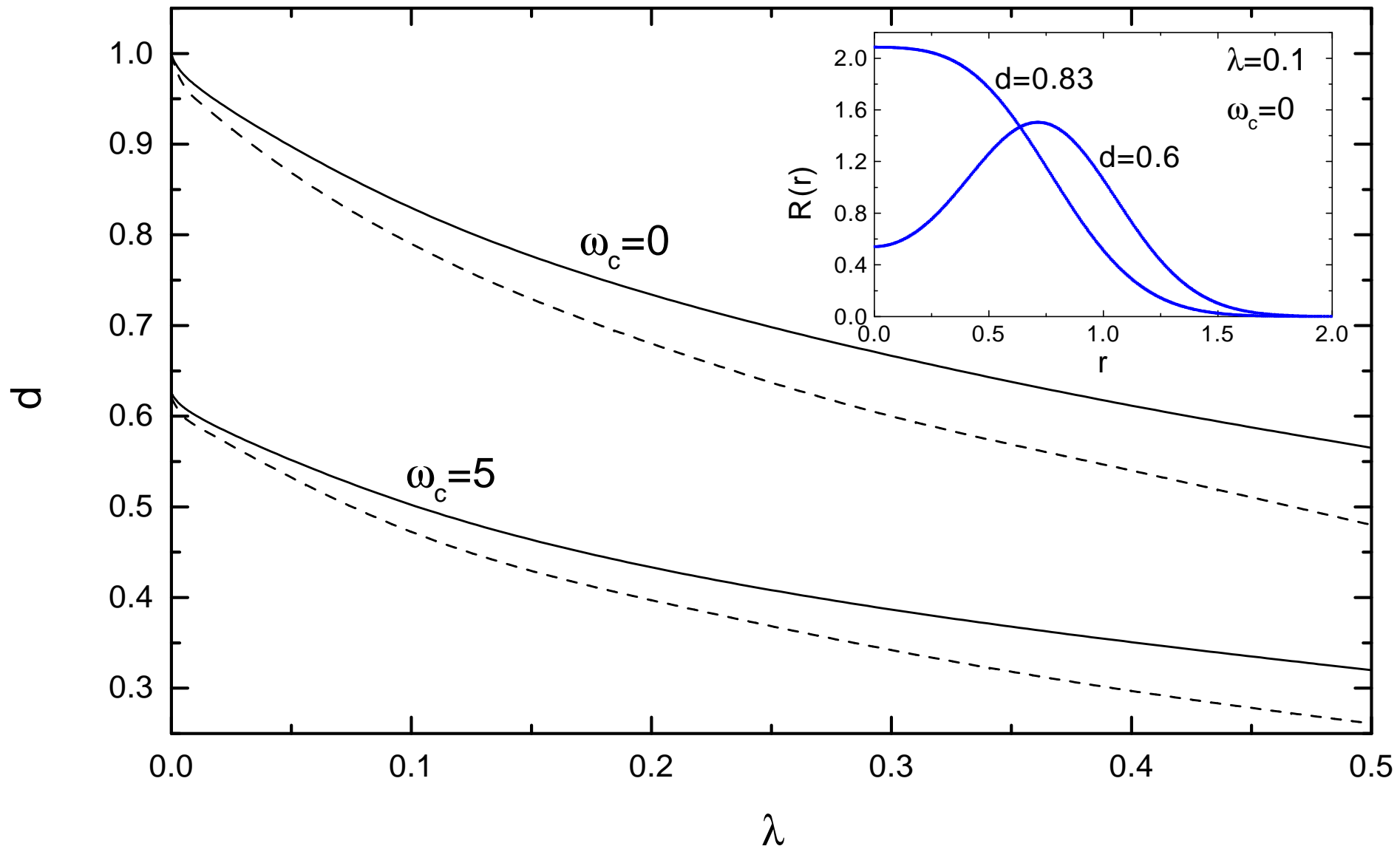


Figure 4

